UC Santa Cruz
UC Santa Cruz Previously Published Works

Title

ATP allosterically activates the human 5-lipoxygenase molecular mechanism of arachidonic acid and 5(S)-hydroperoxy-6(E),8(Z),11(Z),14(Z)-eicosatetraenoic acid.

Permalink

https://escholarship.org/uc/item/8137h3hr

Journal

Authors

Smyrniotis, Christopher
Barbour, Shannon
Xia, Zexin
et al.

Publication Date

DOI

Peer reviewed

ATP Allosterically Activates the Human 5-Lipoxygenase Molecular Mechanism of Arachidonic Acid and 5(S)-Hydroperoxy-6(E),8(Z),11(Z),14(Z)-eicosatetraenoic Acid

Christopher J. Smyrniotis,[†] Shannon R. Barbour,[†] Zexin Xia,[†] Mark S. Hixon,[‡] and Theodore R. Holman*,[†]

[†]Department of Chemistry and Biochemistry, University of California, Santa Cruz, California 95064, United States
[‡]Biological Sciences, Takeda California, Inc., 10410 Science Center Drive, San Diego, California 92121, United States

ABSTRACT: 5-Lipoxygenase (5-LOX) reacts with arachidonic acid (AA) to first generate 5(S)-hydroperoxy-6(E),8(Z),11(Z),14(Z)-eicosa-tetraenoic acid [5(S)-HpETE] and then an epoxide from 5(S)-HpETE to form leukotriene A_4, from a single polyunsaturated fatty acid. This work investigates the kinetic mechanism of these two processes and the role of ATP in their activation. Specifically, it was determined that epoxidation of 5(S)-HpETE (dehydration of the hydroperoxide) has a rate of substrate capture (V_{max}/K_m) significantly lower than that of AA hydroperoxidation (oxidation of AA to form the hydroperoxide); however, hyperbolic kinetic parameters for ATP activation indicate a similar activation for AA and 5(S)-HpETE. Solvent isotope effect results for both hydroperoxidation and epoxidation indicate that a specific step in its molecular mechanism is changed, possibly because of a lowering of the dependence of the rate-limiting step on hydrogen atom abstraction and an increase in the dependency on hydrogen bond rearrangement. Therefore, changes in ATP concentration in the cell could affect the production of 5-LOX products, such as leukotrienes and lipoxins, and thus have wide implications for the regulation of cellular inflammation.
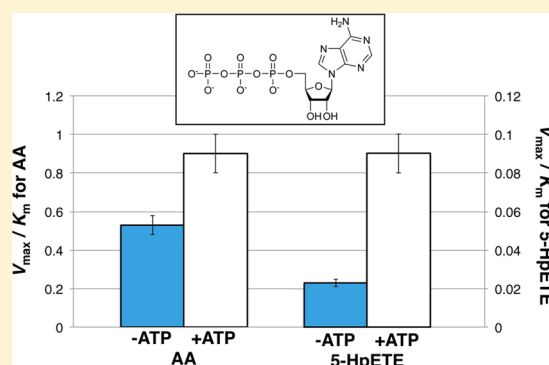
Human 5-lipoxygenase (5-LOX) is a non-heme iron-containing enzyme responsible for catalyzing the stereo-specific and regiospecific peroxidation of natural polyunsaturated fatty acid (PUFA) substrates, specifically converting arachidonic acid (AA) into 5(S)-hydroperoxy-6-*trans*-8,11,14-*cis*-eicosatetraenoic acid [5(S)-HpETE].[1,2] 5-LOX shares this hydroperoxidation activity with other lipoxygenases, such as 12-LOX and 15-LOX, although these generate different products with different biological roles in the cell [e.g., 12(S)-HpETE and 15(S)-HpETE, respectively]. A unique feature of 5-LOX is the additional catalytic step of converting 5(S)-HpETE into the epoxide, leukotriene A_4 (LTA$_4$) (Figure 1). This biomolecule is the first in a line of highly pro-inflammatory mediators that act as potent chemoattractants and are implicated in a variety of diseases from asthma to cancer.[3−6] Distinguishing the biological role of 5-LOX further is the fact that LTA$_4$ can also be shuttled into neighboring cells expressing 12- and 15-LOX via mechanisms of transcellular biosynthesis.[7,8] Ultimately, LTA$_4$ is converted to a series of inflammatory biomolecules (e.g., leukotrienes and lipoxins), both of which are important in initiating and terminating inflammation.[9,10]

5-LOX catalytic activity is regulated through several mechanisms by the cell. 5-LOX is recruited to the nuclear membrane upon cellular Ca^{2+} influx. Calcium binds to allosteric sites in the 5-LOX N-terminal polycystin-1/lipoxygenase/α-toxin (PLAT) domain, promoting attachment to the membrane via conserved tryptophan residues that embed into the lipid
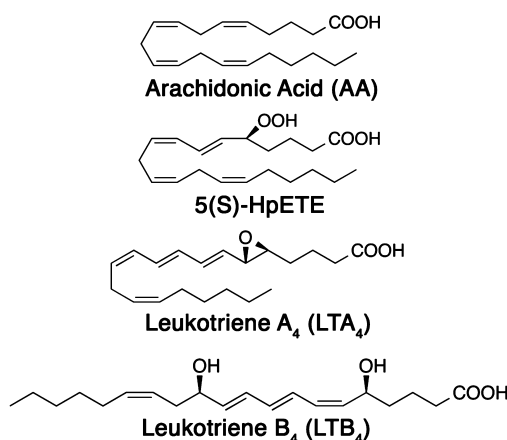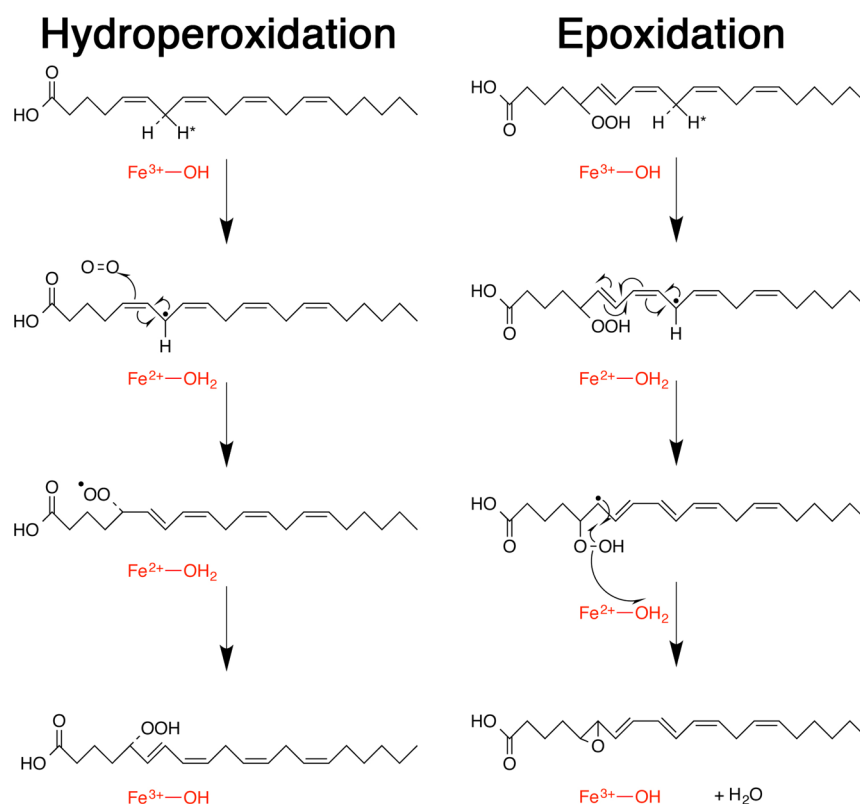

Figure 1. Important metabolites of the regulation of inflammation made by 5-LOX with AA.

bilayer.[11−13] There is also evidence that magnesium can substitute for calcium in this regard.[14] Membrane association leads to an increased level of production of hydroperoxide and leukotriene.[15,16] 5-LOX must interact with 5-LOX-activating

Figure 2. Detailed mechanism of hydroperoxidation and epoxidation [dehydration of 5(*S*)-HpETE to produce the epoxide]. Hydroperoxidation proceeds after initial abstraction of the *pro-S* hydrogen at C7, whereas epoxidation proceeds after abstraction of the *pro-R* hydrogen at C10.[55] The antarafacial nature of hydroperoxidation is well-known,[31,47,79] while a suprafacial arrangement for epoxidation was postulated by Jin et al.[34]

protein (FLAP) to secure PUFA substrates from the nuclear membrane and further promote leukotriene formation *in vivo*.[17,18] Evidence of an additional protein−protein interaction with coactosin-like protein (CLP), an actin binding protein, suggests CLP helps stabilize the membrane-docked 5-LOX and enhances leukotriene formation 3-fold.[19,20] The fate of LTA$_4$ depends on where 5-LOX is localized in the cell when it is activated to bind the nuclear membrane, a phenomenon termed compartmentalization.[21−23] LTA$_4$ can be converted to LTB$_4$ by LTA$_4$ hydrolase, a soluble protein that can localize in the nucleus, or to LTC$_4$ by LTC$_4$ synthase, a membrane-bound protein embedded in the outer leaflet of the nuclear membrane. Compartmentalization implicates the importance of the 5-LOX nuclear localization sequences,[24] which may be further regulated by phosphorylation.[25] Lastly, the ability of 5-LOX to dimerize may provide yet another avenue of enzymatic regulation.[26]

In addition to the calcium binding allosteric sites, there is an ATP binding site(s) that contributes to 5-LOX activation.[27−29] Previous studies report a range of 5-LOX activating potentials, from a 5-fold increase in 5-LOX activity[27] to a 25-fold increase in k_{cat}/K_m with Ca^{2+} added,[30] both found in guinea pig peritoneal polymorphonuclear leukocytes (PMNLs). Furthermore, the substrate specificity of 5-LOX is affected by ATP, with the k_{cat}/K_m ratio of AA to eicosapentaenoic acid (EPA) increasing 2-fold.[30] Unfortunately, the ATP-induced activation mechanism is not thoroughly understood and is often explained with generalized statements, such as extending enzyme stability.[31] The recent crystal structure of Stable-5-LOX, a mutant with a half-life longer than that of wild-type 5-LOX, gave further impetus for characterizing ATP's effect on 5-LOX

because the structural determinants for ATP-induced activation were not obvious from the structure.[32] In addition, it was not known if ATP activated just hydroperoxidation or epoxidation as well.

In comparing the proposed mechanisms of hydroperoxidation (oxidation of AA) and epoxidation (dehydration of the hydroperoxide to form the epoxide), we observed that they are similar but exhibit four key differences (Figure 2). First, the hydrogen atom is abstracted from C7 for hydroperoxidation but from C10 for epoxidation. Therefore, the positioning of the substrate will be distinct between the two processes because the Fe(III)−OH moiety is proposed to be the active species for both abstractions. Second, molecular oxygen does not attack the radical intermediate for epoxidation; rather, there is a radical rearrangement producing the epoxide. Third, the Fe(II)−OH$_2$ moiety donates a hydrogen atom to the peroxyl radical intermediate on C5 for hydroperoxidation but donates a hydrogen atom to a hydroxide radical for epoxidation, which is homolytically cleaved from the hydroperoxide. Finally, these two processes require different substrate rearrangement steps to abstract a hydrogen atom from the substrate and donate it back to the intermediate. It is proposed that after abstraction of a hydrogen atom from C7 and the antarafacial dioxygen attack, the Fe(II)−OH$_2$ moiety transfers an electron, via long range, to the peroxyl radical intermediate.[33] For epoxidation, the hydrogen atom is abstracted from C10; however, the Fe(II)−OH$_2$ moiety is on the same side as the hydroperoxide, leading to a suprafacial homolytic cleavage of the hydroperoxide (Figure 2).[34] This opens the possibility that the homolytic cleavage of the hydroperoxide by the Fe(II)−OH$_2$ moiety to

produce the epoxide could possibly be achieved via an inner sphere reduction, directly with the iron center.

In this report, we determine that ATP allosteric activation of 5-LOX promotes both $5(S)$-HpETE and LTA_4 catalysis by a similar magnitude. ATP induces hyperbolic activation, allowing for the determination of K_i, the strength of ATP binding, α, the change induced in K_m, and β, the change induced in V_{max}. Further kinetic investigations into the solvent and viscosity effects on product formation reveal changes in microscopic rate constants that promote activation, establishing that ATP is an allosteric activator of both 5-LOX hydroperoxidation and epoxidation. Finally, we review the literature on the role of ATP in inflammation and speculate that the ATP-induced allosteric activation of 5-LOX *in vitro* is a potentially relevant modulator of inflammation *in vivo*.

■ MATERIALS AND METHODS

Ammonium Sulfate Precipitation of 5-LOX. Recombinant human 5-LOX in a pET21 plasmid was expressed in *Escherichia coli* BL21(DE3) cells as described previously.[35] Briefly, host cells were grown in LB (100 μg/mL ampicillin) to an OD of 0.6 at 37 °C, at which time they were induced with 0.25 mM IPTG and cooled to 18 °C for overnight growth. Cells were then centrifuged at 4700g for 15 min, pelleted into smaller aliquots at 6200g for 7 min, and snap-frozen in liquid nitrogen. Frozen cell pellets were resuspended in a nitrogen-sparged, 4 °C chilled buffer of 50 mM Hepes and 0.1 mM EDTA (pH 7.5) normalized to an ionic strength of 50 mM with NaCl (termed buffer A in all subsequent methods). A French pressure cell press was used to lyse cells at 2000 psi, and the resulting lysate was centrifuged at 46000g for 25 min. Ammonium sulfate was added to the supernatant [50% (w/v)], and the mixture was inverted to mix, centrifuged at 46000g for 20 min, divided into 200 mg aliquots, and snap-frozen in liquid nitrogen for long-term storage. When needed for enzymatic assays, an aliquot was resuspended in nitrogen-sparged, 4 °C chilled buffer A to a standard concentration and utilized within 3 h to avoid enzyme degradation caused by the inherent instability of 5-LOX.

Purification of LOX Hydroperoxide and Hydroxide Enzymatic Products. High-performance liquid chromatography (HPLC) running solutions were made prior to the experiment. Solution A consisted of 99.9% ACN and 0.1% acetic acid; solution B consisted of 99.9% H_2O and 0.1% acetic acid. AA was used to generate $5(S)$-HpETE. Two liters of 100 μM PUFA substrate in buffer A was reacted with 5-LOX and the reaction run to completion as monitored by a sample reaction on a UV−vis spectrometer; the product was promptly extracted three times with a total volume of dichloromethane of 900 mL, evaporated to dryness, and reconstituted in MeOH for HPLC purification. Products were injected onto a Higgins Haisil Semi-Preparative (5 μm, 250 mm × 10 mm) C-18 column with an elution protocol consisting of a 3 mL/min isocratic mobile phase of 55% solution A and 45% solution B. Both products were tested using analytical HPLC and liquid chromatography and tandem mass spectrometry (LC−MS/MS), demonstrating >90% purity, with the other <10% being hydrolysis products of the hydroperoxide (5-hydroxides and 5-ketones), which were found to be inert when reacted with 5-LOX.

Steady-State Kinetic Measurements. Steady-state kinetic rates were determined by following the formation of the conjugated product at 234 nm [$\varepsilon = 27000$ M^{-1} cm^{-1} for AA

turnover; $\varepsilon = 50000$ M^{-1} cm^{-1} for $5(S)$-HpETE turnover] with a PerkinElmer Lambda 40 UV−vis spectrophotometer at room temperature (21 °C). All assays were conducted in buffer A. AA concentrated stock solutions were stored in 95% ethanol and diluted into buffer so that the total ethanol concentration was <1%. Fatty acid concentrations were verified by full turnover with soybean-1 lipoxygenase and quantitating product concentration. Enzymatic reactions were initiated by the addition of approximately 100−300 nM ammonium sulfate-precipitated wild-type enzyme. The catalytic activity relative to protein weight was measured by observing turnover of a 10 μM solution of AA by the production of $5(S)$-HpETE at 234 nm and was calculated to be ≈0.2 absorbance unit s^{-1} mg^{-1}, or an absolute enzymatic activity of ≈60 μmol min^{-1} mg^{-1} (not standardized to metal content). Activities of all wild-type ammonium sulfate preparations used were within 20% of this value. Assays were conducted in volumes of 2 mL with substrate concentrations ranging from 1 to 30 μM and were constantly stirred with a rotating magnetic bar. Higher substrate concentrations were avoided to prevent the formation of micelles, which would alter the free substrate concentration.[36] Initial rates (up to the first 20% of the reaction) for each substrate were fit to the Michaelis−Menten equation using KaleidaGraph (Synergy) and kinetic parameters calculated. Calculation of V_{max}/K_m parameters was conducted by plotting them as second-order rate constants. All other kinetic parameters (α, β, and K_i) were calculated from fitting data to the equations described by Mogul et al.[37] and Joshi et al.[38] Each plot comprises data from three or four separate experiments, and the reported error is the error calculated from nonlinear regression. Wild-type 5-LOX from the ammonium sulfate preparation showed no inactivation for the 2 h duration of the experiment, and no $5(S)$-HpETE inhibition was observed for the initial rates of AA catalysis. Finally, it should be noted that the ammonium sulfate preparation, without 5-LOX, did not include any fatty acid substrates or impurity proteins with LOX activity.

Measurement of the CMC via Isothermal Titration Calorimetry. CMCs were measured as described by McAuley et al.[39] A MicroCal VP-ITC Calorimeter was used for data collection. A solution of highly concentrated AA, dissolved in buffer A, was titrated into a sample cell containing buffer A only. The final concentration of AA was determined by quantitating the product concentration after full turnover with soybean-1 lipoxygenase, and from this, the molar amount of AA added per injection was extrapolated. Experiments were repeated three times, and the reported error is the standard error of the mean (SEM) of each set of measurements.

HPLC Determination of the $5(S)$-HETE/5,12-DiHETE Product Ratio. 5-LOX prepared by ammonium sulfate precipitation was incubated with 10 μM AA in buffer A at room temperature (21 °C). Enzymatic reactions were quenched with 1% (v/v) glacial acetic acid at varied levels of turnover between 5 and 60%, as determined by UV−vis spectrophotometry. Products were then extracted with dichloromethane, reduced with trimethylphosphite, and evaporated to dryness under a nitrogen stream. The products were purified via HPLC as described above for hydroperoxide products using a Phenomenex Luna (5 μm, 250 mm × 4.6 mm) C-18 column and an elution protocol consisting of a 1 mL/min isocratic mobile phase of 55% solution A and 45% solution B. The molar amounts of $5(S)$-HETE and 5,12-DiHETE were calculated by the corresponding peak areas determined by

Table 1. Steady State Parameters of 5-LOX Hydroperoxidation of AA and Epoxidation of 5(S)-HpETE, with and without ATP

[ATP] (μM)	AA hydroperoxidation			5(S)-HpETE epoxidation		
	relative V_{max}[a]	K_m (μM)	relative V_{max}/K_m	relative V_{max}	K_m (μM)	relative V_{max}/K_m
0	1.0 ± 0.02	1.9 ± 0.2	0.53 ± 0.05	0.33 ± 0.01	14 ± 1	0.023 ± 0.002
200	4.9 ± 0.3	5.3 ± 0.8	0.90 ± 0.1	1.6 ± 0.09	19 ± 2	0.090 ± 0.01
ATP change	4.9-fold		1.7-fold	4.8-fold		3.9-fold

[a]The relative V_{max} of 5-LOX (ammonium sulfate-precipitated) and AA, with no cofactors added, is set to 1. All other V_{max} values are standardized to this value and are unitless. V_{max} values with 5(S)-HpETE as a substrate were multiplied by 0.54 to account for the difference in extinction coefficients between HETE (234 nm) and diHETE (280 nm) products. For comparison to other studies, the absolute kinetic activity of all of our wild-type 5-LOX preparations, without ATP added, was ≈60 μmol min^{-1} mg^{-1}.

HPLC and normalized to their respective extinction coefficients (ε_{234} = 27000 M^{-1} cm^{-1}, and ε_{280} = 50000 M^{-1} cm^{-1}).[40,41] Reactions were repeated 12−26 times, and the reported error is the SEM of each set of measurements.

Structural Determination of 5-LOX-Catalyzed Products by LC−MS/MS. LC−MS/MS running solutions were made prior to each experiment. Solution A consisted of 99.9% H$_2$O and 0.1% formic acid; solution B consisted of 99.9% ACN and 0.1% formic acid. Ammonium sulfate-precipitated 5-LOX was incubated with 10 μM AA substrate. A 2 mL sample of the reaction mixture was monitored at 234 nm with a PerkinElmer Lambda 40 UV−vis spectrophotometer to determine when complete turnover had been reached. Reactions were quenched with 1% (v/v) glacial acetic acid, extracted with dichloromethane, reduced with trimethylphosphite, evaporated to dryness, and reconstituted in MeOH. Products were injected onto a Phenomenex Synergi (4 μm, 150 mm × 4.6 mm) C-18 column attached to a Finnigan LTQ liquid chromatography mass spectrometer (LC−MS/MS). The elution protocol consisted of 200 μL/min, with an isocratic mobile phase of 40% solution A and 60% solution B. The corresponding reduced product ion peak ratio was determined using negative ion MS/MS (collision energy of 35 eV) with the following masses: 5(S)-HETE, parent ion at m/z 319 and fragments at m/z 115, 203, and 129; 5,12-DiHETE, parent ion at m/z 335 and fragments at m/z 317, 273, and 195.[42,43]

^{18}O Labeling of PUFA Substrates. HPLC running solutions were made prior to each experiment. Solution A consisted of 99.9% MeOH and 0.1% acetic acid; solution B consisted of 99.9% H$_2$O and 0.1% acetic acid. Arachidonoyl chloride and eicosapentaenoyl chloride (>99%) were purchased from Nu-Chek Prep, Inc. H$_2$^{18}O (97%) was purchased from Cambridge Isotope Laboratories. One molar equivalent of acyl chloride substrate was reacted with 15 molar equiv of H$_2$^{18}O in the presence of dried pyridine for 10 min in a nitrogen-sparged flask. Lipids were extracted twice with dichloromethane, evaporated to dryness, and reconstituted in MeOH for HPLC purification. The sample was injected onto a Higgins Haisil Semi-Preparative (5 μm, 250 mm × 10 mm) C-18 column and eluted with an isocratic program of 75% solution A and 25% solution B. The substrate purity was calculated to be greater than 99% on an LC−MS/MS, although we measured a range of ^{18}O labeling efficiencies from 57 to 78% in different labeling experiments. Isotope ratios of labeled to unlabeled PUFA substrate were used to normalize the data.

Competitive Substrate Capture Investigations of PUFA and Hydroperoxide Catalysis. LC−MS/MS running solutions were made prior to each experiment. Solution A consisted of 99.9% H$_2$O and 0.1% formic acid; solution B consisted of 99.9% ACN and 0.1% formic acid. Competitive substrate capture method experiments were performed using a reaction mixture of labeled PUFA substrate and its respective hydroperoxide product [[^{18}O]AA/5(S)-HpETE] with a known molar ratio (1:1) and were initiated with ammonium sulfate-precipitated 5-LOX in buffer A in the presence or absence of 200 μM ATP. The ratio of the simultaneous product formation (5,12-[^{18}O]dihydroxides and 5,12-dihydroxides) by 5-LOX was determined at a total substrate concentration of 1 μM (substrate limiting conditions). A 2 mL sample of the reaction mixture was monitored at 234 nm with a PerkinElmer Lambda 40 UV−vis spectrophotometer to determine time points to achieve ∼5% total substrate consumption (∼0.05 μM).[27,44] Reactions were timed and quenched with 1% glacial acetic acid (v/v), and mixtures were extracted with dichloromethane, reduced with trimethylphosphite, evaporated to dryness, and reconstituted in MeOH. Products were injected onto a Phenomenex Synergi (4 μm, 150 mm × 4.6 mm) C-18 column attached to a Finnigan LTQ liquid chromatography tandem mass spectrometer (LC−MS/MS). The elution protocol consisted of 200 μL/min, with an isocratic mobile phase of 40% solution A and 60% solution B. The corresponding reduced product ion peak ratio was determined using negative ion MS/MS (collision energy of 35 eV) with the following masses: 5,12-DiHETE, parent ion at m/z 335 and fragments at m/z 317, 273, and 195; 5,12-[^{18}O]DiHETE, parent ion at m/z 337 and fragments at m/z 319, 273, and 197.[42] The ratio of the peak areas for the labeled and unlabeled dihydroxides was then used to determine the $(V_{max}/K_m)^{AA}/(V_{max}/K_m)^{5(S)\text{-HpETE}}$ ratio, modeled after our previous report.[44] Reactions were repeated 14−21 times, and the reported error is the SEM of each set of measurements.

Measurement of Solvent Isotope Effects. Steady-state kinetics were performed in H$_2$O and ^{2}H$_2$O at room temperature (21 °C) as previously described to reveal SIEs.[45,46] Reactions were performed in buffer A (H$_2$O, pH 7.5) or in the same buffer made with ^{2}H$_2$O (pH meter reading of 7.1[47]), and all kinetic parameters were determined as described above. A Hewlett-Packard diode-array 8453 UV−vis spectrometer was used to simultaneously observe 5(S)-HpETE and LTA$_4$ formation and thus determine the SIE for either step of catalysis.

Measurement of Viscosity Effects. Steady-state kinetics were performed in the absence or presence of a viscogen (dextrose) at room temperature (21 °C) to reveal any diffusion-linked effects on catalysis as previously described.[46,48] Maltose, sucrose, ethylene glycol, glycerol, trimethylamine N-oxide (TMAO), and PEG-8000 were also tested as viscogens, but all of these inhibited (>50%) enzymatic catalysis and thus were not further used. Reactions were conducted at different relative viscosities ($\eta_{rel} = \eta/\eta_0$, where η_0 is the viscosity of H$_2$O at 20 °C) in 25 mM Hepes and 0.05 mM EDTA (pH 7.5), normalized to an ionic strength of 25 mM with NaCl. All

kinetic parameters were determined as described above in the absence ($\eta_{rel} = 1$) or presence of 1.873 M dextrose ($\eta_{rel} = 3$).

■ RESULTS AND DISCUSSION

Steady-State Kinetic Dependence on ATP and Ca²⁺. Steady-state hydroperoxidation kinetics of AA demonstrated that the addition of a saturating level of ATP (200 μM) produced a 4.9-fold increase in V_{max} and a 1.7-fold increase in V_{max}/K_m. This increase is due to a large increase in V_{max}, relative to a small increase in K_m (Table 1), indicating that ATP increases the rate of product release more so than substrate capture. These observations are consistent with the ATP activation reported by Ochi et al. for 5-LOX purified from guinea pig neutrophils,[27] underscoring a similarity between the ATP activation of human and guinea pig 5-LOX isozymes. It should be noted that Aharony et al. observed a decrease in K_m upon addition of Ca²⁺ and ATP, leading to an increase in k_{cat}/K_m (25-fold) larger than what we observed.[30] We infrequently saw a decrease in K_m, as well, but it was only with a small percentage of our 5-LOX preparations; therefore, we did not consider it relevant. Interestingly, these infrequent preparations of 5-LOX, which demonstrated a decrease in K_m, also exhibited substrate inhibition and manifested artificially lower K_m values. This substrate inhibition was not due to a change in the critical micelle concentration (CMC) for AA because the substrate concentrations used were well below the CMC values [CMC = 43 ± 3 μM (no ATP) and 52 ± 1 μM (200 μM ATP)], as measured by isothermal titration calorimetry. In addition, it was confirmed with our 5-LOX preparation that calcium was not required for ATP activation (data not shown), as previously reported with recombinant human 5-LOX, obtained from insect cell expression.[31,49] However, we did notice that calcium slightly diminished the level of ATP activation (~10%), but the cause of this small reduction in the level of activation is unclear. 1,2-Dimyristoyl-*sn*-glycero-3-phosphocholine (DMPC), with and without Ca²⁺ and/or Mg²⁺, also showed no observable kinetic effect on ATP activation. Furthermore, DMPC hindered accurate absorption detection because of its high background absorption, and thus, it was not included in further experiments (data not shown).

Steady-state epoxidation kinetics of 5(S)-HpETE demonstrated a 3-fold smaller V_{max} and a 23-fold smaller V_{max}/K_m, compared to those for hydroperoxidation of AA (Table 1). These results highlight a prominent difference between AA and 5(S)-HpETE in their rates of substrate capture and suggest that LTA₄ formation could occur more readily from sequential steps of hydroperoxidation and then epoxidation with AA, as has been previously observed.[40,50] The addition of a saturating level of ATP (200 μM) produced a 4.8-fold increase in V_{max} with 5(S)-HpETE as the substrate, which was the same magnitude of activation seen for AA hydroperoxidation (Table 1). In contrast, ATP induced a 3.9-fold increase in V_{max}/K_m, which indicates a 2-fold greater ATP-induced activation of V_{max}/K_m for 5(S)-HpETE epoxidation than for AA hydroperoxidation (1.7-fold). These data demonstrate a distinction in the ATP activation mechanism for hydroperoxidation and epoxidation, and therefore, more extensive investigations were used to understand ATP activation in more detail.

Effect of ATP-Induced Activation on Hydroperoxide Retention and Epoxide Formation. As described above, ATP activates both AA hydroperoxidation and 5(S)-HpETE epoxidation. However, it is unclear if the epoxidation reaction affects the rate of hydroperoxidation, because of the

consumption of the hydroperoxidation product, 5(S)-HpETE, and/or production of the 5,6-epoxide, LTA₄. To investigate this possibility, a diode-array UV−vis spectrophotometer was used to observe the formation of both 5(S)-HpETE (234 nm) and LTA₄ (280 nm) simultaneously from 0 to 20% product formation and determine if the slight increase in the 5(S)-HpETE concentration could affect the rate of hydroperoxide formation. The LTA₄/5(S)-HpETE ratio of products (the efficiency of epoxide formation) was calculated throughout the reaction and observed to remain constant up to 20% product formation [LTA₄/5(S)-HpETE ratio of 0.161 ± 0.004 (Figure 3)]. With the addition of 200 μM ATP, this value increased to a
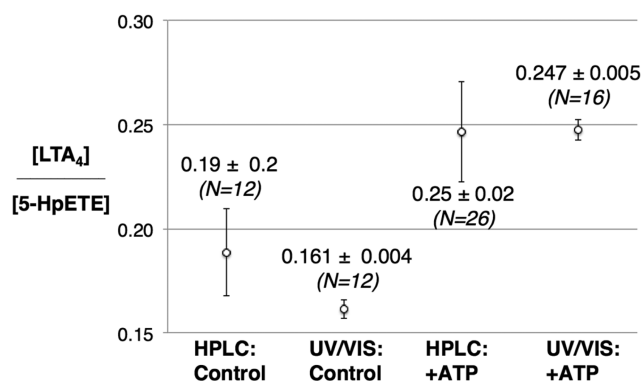
Figure 3. Effect of 200 μM ATP on the efficiency of epoxide formation. [LTA₄]/[5(S)-HpETE] turnover ratio from 10 μM AA substrate as measured by HPLC and UV−vis spectrophotometry. [LTA₄] was measured at 280 nm and [5(S)-HpETE] at 234 nm, and both were normalized to their respective extinction coefficients. The absolute kinetic activity of wild-type 5-LOX ammonium sulfate preparations was ≈60 μmol min⁻¹ mg⁻¹.

constant value of 0.247 ± 0.005 (Figure 3) and matched the value determined for rat PMNL 5-LOX.[40] In addition, 5(S)-HETE and 5,12-DiHETE concentrations were quantified via HPLC and comparable product ratios were observed [0.19 ± 0.02 (no ATP) and 0.25 ± 0.02 (200 μM ATP)], confirming the accuracy of the dual-wavelength assay (Figure 3). These data indicate that the consumption of 5(S)-HpETE, and the subsequent production of the 5,6-epoxide, does not affect the relative rates of hydroperoxidation and epoxidation.

Hyperbolic Activation of 5-LOX by ATP. To compare the allosteric effect of ATP activation for AA hydroperoxidation and 5(S)-HpETE epoxidation in more detail, extensive allosteric titrations were performed (Table 2). From the data,

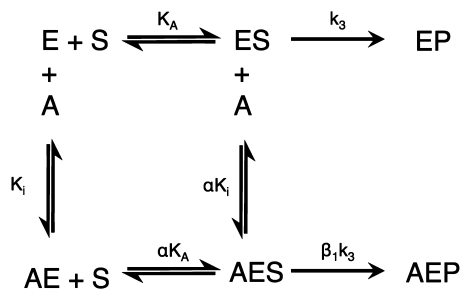**Table 2. Kinetic Parameters for ATP-Induced Activation of 5-LOX[a]**

substrate	α	β	β/α	K_i (μM)
AA	3.0 ± 0.4	5.4 ± 0.08	1.8 ± 0.2	8.0 ± 6
5(S)-HpETE	1.6 ± 0.08	5.1 ± 0.1	3.3 ± 0.2	12 ± 5

[a]Hyperbolic fit parameters of 5-LOX with ATP and AA or 5(S)-HpETE as substrates.

it was observed that 5-LOX and AA exhibited a hyperbolic response to increasing amounts of ATP with an increase in K_m(app) from 1.9 ± 0.2 to 5.3 ± 0.8 μM and an increase in V_{max}/K_m(app) from 0.53 ± 0.05 to 0.9 ± 0.1. The saturation behavior of K_m(app) and V_{max}/K_m, with AA as the substrate, is indicative of hyperbolic activation (i.e., partial activation).

Similar hyperbolic allostery has been observed for other LOX isozymes with different allosteric regulators, such as soybean 15-LOX-1 with oleyl sulfate[37] and human 15-LOX-2 with 13(S)-HODE.[38] These data indicate the presence of an allosteric binding site in 5-LOX that affects the catalysis by changing the microscopic rate constants of 5-LOX, as described in Scheme 1. From Scheme 1, eqs 1−4 allow for the

Scheme 1. Kinetic Scheme for Allosteric Activation of 5-LOX[a]

$$E + S \xrightleftharpoons{K_A} ES \xrightarrow{k_3} EP$$

$$+ \qquad +$$
$$A \qquad A$$

$$K_i \qquad \alpha K_i$$

$$AE + S \xrightleftharpoons{\alpha K_A} AES \xrightarrow{\beta_1 k_3} AEP$$

[a]5-LOX catalysis including hyperbolic partial activation induced by ATP. Similar hyperbolic allostery has been observed for other LOX isozymes with different allosteric regulators, such as soybean 15-LOX-1 with oleyl sulfate[37] and human 15-LOX-2 with 13(S)-HODE.[38]

Figure 4. Effect of ATP on the K_m(app) of 5-LOX with the AA substrate. The data are fit to eq 2 (Scheme 1), where K_m = 1.9 μM. α and K_i were determined to be 3.0 $\pm$ 0.4 and 8.0 $\pm$ 6 μM, respectively.

determination of K_i, the strength of binding, α, the change in K_m, β, the change in V_{max}, and β/α, the change in V_{max}/K_m.

$$1/\nu = (\alpha K_m/V_{max}) \times [([I]+K_i)/(\beta[I]+\alpha K_i)]$$
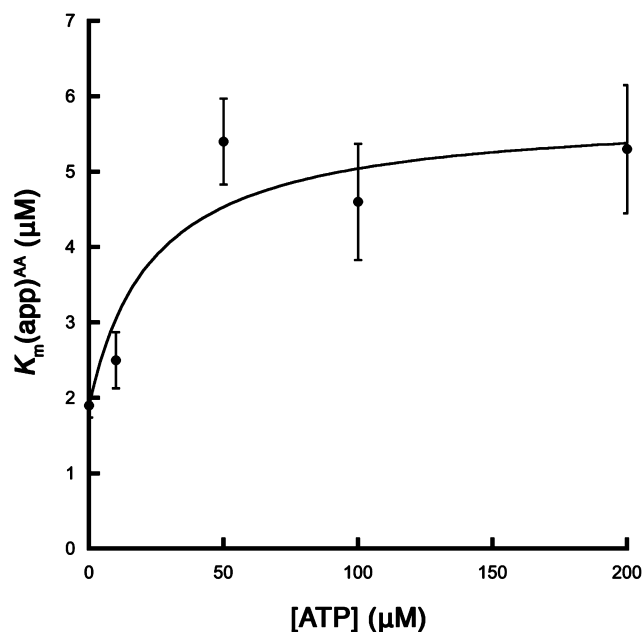$$\times 1/[S] + 1/V_{max} \times [([I]+\alpha K_i)/(\beta[I]+\alpha K_i)] \quad (1)$$

$$K_m(\text{app}) = \alpha K_m[([I]+K_i)/([I]+\alpha K_i)] \quad (2)$$

$$V_{max}/K_m(\text{app}) = (V_{max}/\alpha K_m) \times [(\beta[I]+\alpha K_i)/([I]+K_i)] \quad (3)$$

$$V_{max}(\text{app}) = V_{max}[(\beta[I]+\alpha K_i)/([I]+\alpha K_i)] \quad (4)$$

A plot of K_m(app) versus ATP concentration, with AA as the substrate (Figure 4), yielded an α of 3.0 $\pm$ 0.4 and a K_i of 8 $\pm$ 6 μM, when fit with eq 2 (Table 2). The values of α and K_i were then utilized in eq 3 and fit to the V_{max}/K_m data, which yielded a β of 5.5 $\pm$ 0.5. The value of β was also determined from the V_{max} data (fit with eq 4 and the values of α and K_i given above), which yielded a β of 5.4 $\pm$ 0.08 (Figure 5) and matched well with the β value from the V_{max}/K_m plot. These values indicate mixed hyperbolic allostery [$\alpha > 1$ (K-type inhibition), and $\beta > 1$ (V-type activation)],[51] with the majority of the kinetic change being seen in the value of V_{max}. This larger V_{max} change is best observed by considering the V_{max}/K_m value, which is greater than 1 (β/α = 1.8 $\pm$ 0.2) and indicates V_{max}/K_m allosteric activation. These hyperbolic data suggest the formation of a catalytically active ternary complex (A·E·S) between 5-LOX and ATP and are consistent with the previous finding of an allosteric site in 5-LOX.[31,52] The data are also consistent with what was observed at saturating ATP concentrations (listed in Table 1).

Similar ATP titration experiments were also performed with 5(S)-HpETE as the substrate, which showed an α value of 1.56 $\pm$ 0.08 (K-type inhibition) and a K_i value of 12 $\pm$ 5 μM (Table 2), from the K_m(app) plot (Figure 6). The α value was half the α value for AA activation, indicative of a weaker ATP allosteric effect on K_m with 5(S)-HpETE as the substrate. However, the
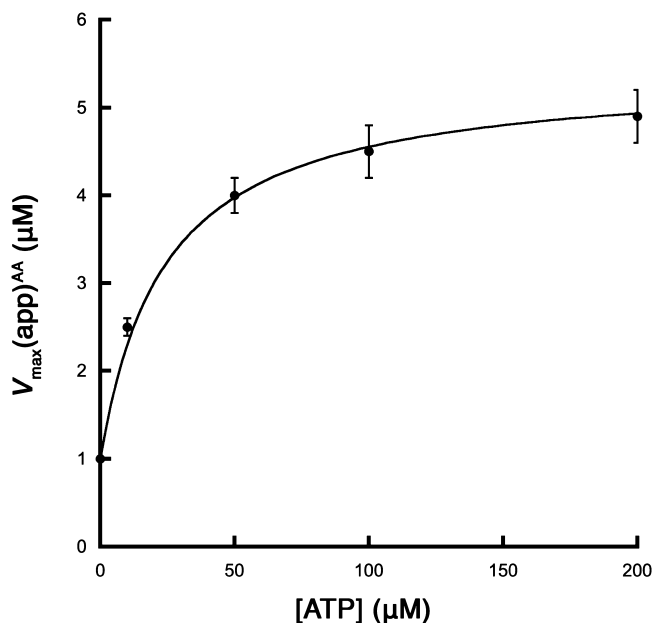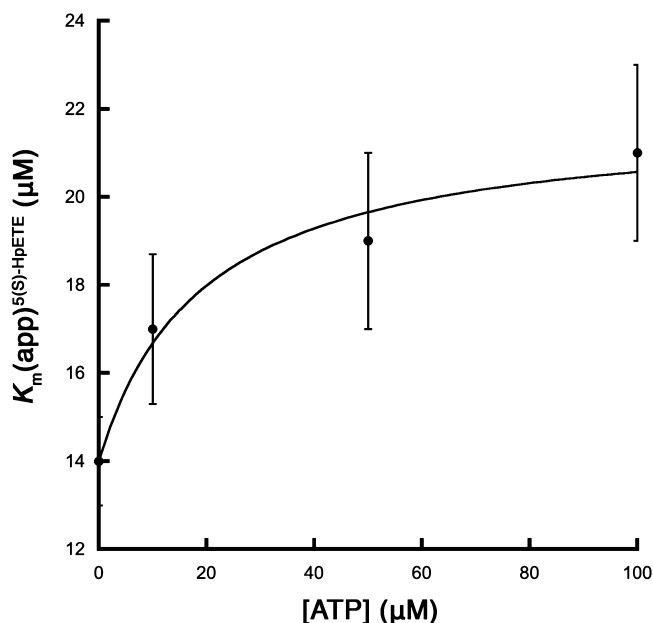
Figure 5. Effect of ATP on the V_{max}(app) of 5-LOX with the AA substrate. The data are fit to eq 4 (Scheme 1) with a K_m of 1.9 μM, an α of 3, and a K_i of 8, where β was determined to be 5.4 $\pm$ 0.08.

K_i value was comparable to that of AA activation, indicating similar ATP binding affinities and most likely the same ATP binding site for both hydroperoxidation and epoxidation. The β value was determined to be 5.1 $\pm$ 0.1 (Figure 7), which is V-type activation, similar to that seen for AA. The β/α ratio is nearly 2-fold greater for 5(S)-HpETE (3.3 $\pm$ 0.2) than for AA (1.8 $\pm$ 0.2), indicating that ATP activates the rate of substrate capture for 5(S)-HpETE more so than AA. These results agree with our kinetic results at saturating ATP concentrations (Table 1), suggesting that the allosteric effect caused by ATP binding has largely similar consequences for both the
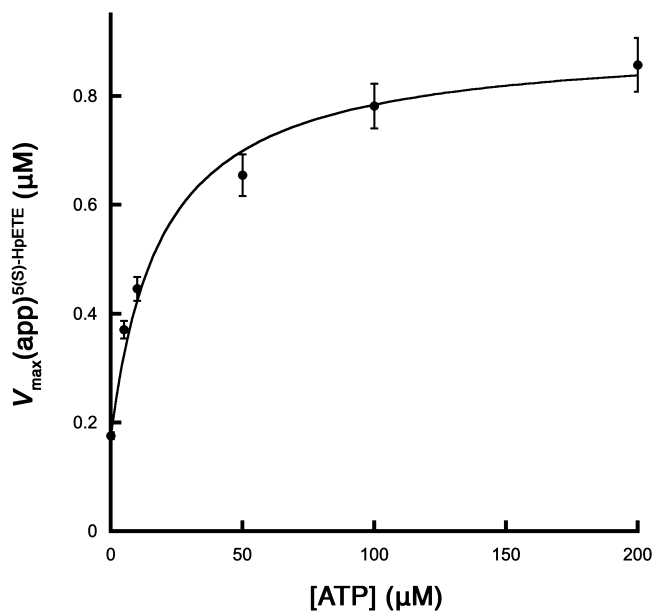
Figure 6. Effect of ATP on the $K_m(app)$ of 5-LOX with the 5(S)-HpETE substrate. The data are fit to eq 2 (Scheme 1), with a K_m of 14 μM. α and K_i were determined to be 1.6 ± 0.08 and 12 ± 5 μM, respectively.

Figure 7. Effect of ATP on the $V_{max}(app)$ of 5-LOX with the 5(S)-HpETE substrate. The data are fit to eq 4 (Scheme 1) with a K_m of 14 μM, an α of 1.6, and a K_i of 12, where β was determined to be 5.1 ± 0.1.

hydroperoxidation of AA and the epoxidation of 5(S)-HpETE, but with subtle differences in magnitude.

Endogenous and Exogenous Rates of Epoxide Formation. As mentioned above, 5-LOX can produce LTA$_4$ from AA sequentially [first producing 5(S)-HpETE and then LTA$_4$] or from 5(S)-HpETE directly. To improve our understanding of the kinetic differences between endogenous 5(S)-HpETE epoxidation (generated *in situ* from AA) and exogenous 5(S)-HpETE epoxidation [binding 5(S)-HpETE directly], steady-state experiments with AA and 5(S)-HpETE as

substrates were performed by indirectly observing epoxide formation from its decomposition product at 280 nm (5,12-diHETE). From Table 3, it is observed that the V_{max} values of epoxidation for both AA and 5(S)-HpETE were the same. This implies that hydrogen abstraction is a dominant rate-limiting step for V_{max} of epoxidation because 5-LOX abstracts the same hydrogen atom from 5(S)-HpETE for epoxidation (C10), regardless of whether the 5(S)-HpETE is endogenous (generated *in situ*) or exogenous (bound directly) (Figure 2). In contrast to the V_{max} data, the V_{max}/K_m for epoxidation of endogenous 5(S)-HpETE was found to be 9-fold larger than the V_{max}/K_m for epoxidation of exogenous 5(S)-HpETE. Considering that both endogenous and exogenous 5(S)-HpETE share the same hydrogen abstraction step, these data indicate there is a difference in their rate-limiting steps prior to hydrogen atom abstraction. A saturating level of ATP (200 μM) activated the V_{max} and the V_{max}/K_m for both endogenous 5(S)-HpETE and exogenous 5(S)-HpETE epoxidation, as would be expected; however, there were slight differences. ATP increased the V_{max} of endogenous 5(S)-HpETE 6.5-fold, relative to 4.8-fold for exogenous 5(S)-HpETE. ATP increased the V_{max}/K_m of endogenous 5(S)-HpETE 2.4-fold, relative to 3.9-fold for exogenous 5(S)-HpETE. The overall similarity in the ATP activation of endogenous and exogenous 5(S)-HpETE is indicative of similar mechanisms. However, the slight differences in ATP activation between endogenous and exogenous 5(S)-HpETE could be due to slight differences in their microscopic rate constants or possibly experimental error.

Competitive Substrate Capture Investigations of AA and 5(S)-HpETE Catalysis. To further investigate the kinetics of AA and 5(S)-HpETE catalysis, a competitive substrate capture experiment was performed with a mixture of [^{18}O]AA (0.5 μM) and unlabeled 5(S)-HpETE (0.5 μM). The results without ATP demonstrated that the amount of 5,12-DiHETEs produced from [^{18}O]AA was larger than the amounts produced from exogenous 5(S)-HpETE, with a measured $(V_{max}/K_m)^{AA}/(V_{max}/K_m)^{5(S)\text{-}HpETE}$ epoxide efficiency ratio of 1.8 ± 0.06. These results confirm the steady-state results (*vide supra*) that 5-LOX is more likely to retain the nascent 5(S)-HpETE in its active site than to bind exogenous 5(S)-HpETE to generate the epoxide. The competitive experiment was repeated with a saturating level of ATP (200 μM), and the $(V_{max}/K_m)^{AA}/(V_{max}/K_m)^{5(S)\text{-}HpETE}$ ratio increased to 2.2 ± 0.06, indicating an increase in the epoxide efficiency of AA conversion, relative to that of 5(S)-HpETE conversion. This is in contrast to the steady-state $(V_{max}/K_m)^{AA}/(V_{max}/K_m)^{5(S)\text{-}HpETE}$ ratio, which not only is larger than the competitive ratio (ratio of 8.6) but also decreases with the addition of ATP (ratio of 6.4). These differences between the two methods could be due to the fact that the competitive measurements were performed with both substrates present while the steady-state experiments included only one substrate at a time. As seen previously for 15-LOX-1 and 15-LOX-2,[37,38] differences between competitive and steady-state measurements can be indicative of allosteric effects by either the substrate or product. Therefore, while these data confirm that the majority of LTA$_4$ produced by 5-LOX is made from AA and not 5(S)-HpETE, additional experiments are required to investigate why the steady-state and competitive methods do not correlate. For comparison, Puustinen et al. observed a $(V_{max}/K_m)^{AA}/(V_{max}/K_m)^{5(S)\text{-}HpETE}$ epoxide efficiency ratio of approximately 3.2 for 5-LOX from the human leukocyte homogenate, with ATP being present,[50] while Wiseman et al. measured a $(V_{max}/K_m)^{AA}/(V_{max}/K_m)^{5(S)\text{-}HpETE}$ ratio of 32 ± 1

Table 3. Steady State Parameters of 5-LOX Epoxidation of AA (Endogenous) and Epoxidation of 5(*S*)-HpETE (Exogenous), with and without ATP

[ATP] (μM)	AA epoxidation (endogenous)			5(*S*)-HpETE epoxidation (exogenous)		
	relative V_{max}[a]	K_m (μM)	relative V_{max}/K_m	relative V_{max}	K_m (μM)	relative V_{max}/K_m
0	0.31 ± 0.01	1.6 ± 0.3	0.18 ± 0.04	0.33 ± 0.01	14 ± 1	0.023 ± 0.002
200	2.0 ± 0.1	4.5 ± 0.7	0.44 ± 0.06	1.6 ± 0.09	19 ± 2	0.090 ± 0.01
ATP change	6.5-fold		2.4-fold	4.8-fold		3.9-fold

[a]The V_{max} of 5-LOX epoxidation of AA (endogenous), with no cofactors added, is normalized to the V_{max} of 5-LOX hydroperoxidation of AA (Table 1). The values for 5(*S*)-HpETE epoxidation (exogenous) from Table 1 are listed again for clarity. For comparison to other studies, the absolute kinetic activity of all of our wild-type 5-LOX preparations, without ATP added, was ≈ 60 μmol/min/mg.

for 5-LOX from rat PMNLs in the presence of ATP,[40] indicating possible differences between species.

Solvent Effects of the Hydroperoxidation and Epoxidation Kinetics. The mechanism of hydroperoxidation for soybean 15-LOX,[47,53] human 12-LOX,[45,46] human 15-LOX-1,[45,46] and human 15-LOX-2[48] has been shown previously to manifest multiple rate-limiting steps, defined by substrate diffusion, hydrogen bond rearrangement, and hydrogen atom abstraction. However, the mechanisms employed by 5-LOX for hydroperoxidation and epoxidation are less well understood.[30,40] The 5-LOX mechanism for hydroperoxidation has historically been assumed to be similar to that of other lipoxygenases,[54] but little experimental evidence has been found. The epoxidation reaction is also proposed to proceed through a hydrogen atom abstraction mechanism, similar to that of hydroperoxidation,[34] which is supported by a large primary kinetic isotope effect of >10,[6,55,56] and inhibition of LTA$_4$ formation by reductive inhibitors.[4] On the basis of the data described above, a scheme has been generated to represent the general steps of hydroperoxidation and epoxidation (Scheme 2). The scheme includes rearrangement steps (k_3

Scheme 2. Kinetic Scheme for 5-LOX Hydroperoxidation and Epoxidation (Dehydration)[a]

[a]5-LOX catalysis proceeds with hydroperoxidation of AA to 5(*S*)-HpETE and either product release or subsequent epoxidation (dehydration) to LTA$_4$. This is based on a scheme originally published by Wiseman et al.[40] The final step (k_{11}) includes both chemical and release steps.

and k_7) and hydrogen atom abstraction steps (k_5 and k_{11}) for both hydroperoxidation and epoxidation, respectively. It should be noted that k_{11} includes both abstraction and product release. With respect to ATP activation, previous work did not determine if molecular steps in the reaction coordinate for either hydroperoxidation or epoxidation are accelerated (Figure 2) or if activation proceeds through an alternative process that does not affect the catalytic mechanism, such as protein stabilization.[31]

In the work presented here, hydroperoxidation kinetic studies of AA in the absence of ATP revealed a normal solvent

isotope effect (SIE) for V_{max}[AA] (1.8 ± 0.2) and an inverse SIE for V_{max}/K_m[AA] (0.66 ± 0.3) (Table 4). Under ATP
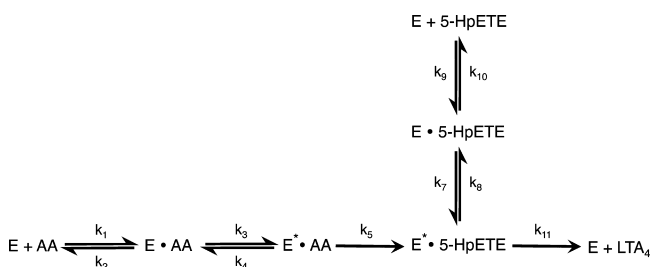
Table 4. Solvent Isotope Effect (SIE) Values for Hydroperoxidation of AA and Epoxidiation of 5(*S*)-HpETE

[ATP] (μM)	AA hydroperoxidation (234 nm)		5(*S*)-HpETE epoxidation (280 nm)	
	V_{max} SIE	V_{max}/K_m SIE	V_{max} SIE	V_{max}/K_m SIE
0	1.8 ± 0.2	0.66 ± 0.3	0.81 ± 0.1	0.49 ± 0.09
200	3.1 ± 0.6	1.8 ± 0.6	2.6 ± 0.3	1.2 ± 0.2

activation (200 μM ATP), the normal SIE increased for V_{max}[AA] to 3.1 ± 0.6, while the inverse SIE for V_{max}/K_m[AA] changed to a normal SIE of 1.8 ± 0.6, demonstrating that ATP affects the molecular mechanisms of both substrate capture and product release. In general, SIE values of 2−3 typically correspond to general acid/base catalysis, while the extent of solvation of catalytic bridges ranges from 1.5 to 4.[57,58] Previous studies of LOX isozymes[45−48,53] attribute their observed SIE results to a solvent-dependent hydrogen transfer from multiple hydrogen bond rearrangements, presumably because of an enzymatic conformational change upon substrate binding. Interestingly, although all four LOX isozymes manifested SIEs, their magnitude and temperature dependence varied, indicating subtle differences in their rate-limiting steps. For 5-LOX, the magnitude of the normal SIE for V_{max}[AA], with and without ATP added, indicates a hydrogen bond rearrangement step (i.e., general conformational change), similar to that seen for other LOX isozymes. The increase in the normal V_{max} SIE value, with addition of ATP, indicates that the hydrogen bond rearrangement step becomes more rate-limiting with added ATP and that the activation of 5-LOX by ATP is in part due to a change in its microscopic rate constants, such as increasing the rate of hydrogen atom abstraction (*vide infra*). It should be noted that lower values of SIE (<1.5) are typically ascribed to proton transfer coupled to heavy atom motion in the transition state[59] or to increased viscosity of D$_2$O relative to H$_2$O.[60] These are unlikely explanations for our data, given their larger SIE values.

In contrast to the V_{max} SIE, the V_{max}/K_m of AA manifests an inverse SIE without ATP (SIE = 0.66 ± 0.3), which becomes a normal SIE (SIE = 1.80 ± 0.61) upon addition of ATP. Previously, our laboratory observed inverse SIE values for both V_{max} and V_{max}/K_m for a soybean 15-LOX mutant[61] and wild-type 15-LOX-2,[48] which was ascribed to the participation of a ferric−hydroxide moiety in the abstraction of the hydrogen atom. It is possible that the observed inverse SIE for 5-LOX with AA is also due to the ferric−hydroxide moiety; however, because of its large error, it is difficult to state this with certainty. Nonetheless, the change to a normal SIE upon

Table 5. Viscosity Effect Values for Hydroperoxidation of AA and Epoxidiation of 5(S)-HpETE

[ATP] (μM)	AA hydroperoxidation (234 nm)		5(S)-HpETE epoxidation (280 nm)	
	V_{max}°/V_{max}	$(V_{max}/K_m^{\circ})/(V_{max}/K_m)$	V_{max}°/V_{max}	$(V_{max}/K_m^{\circ})/(V_{max}/K_m)$
0	1.0 ± 0.1	1.5 ± 0.3	1.0 ± 0.2	0.65 ± 0.1
200	1.6 ± 0.2	1.2 ± 0.2	1.3 ± 0.2	1.6 ± 0.4

addition of ATP is significant and indicates a shift in the nature of the rate-determining step, possibly from a dependence on hydrogen atom abstraction by the ferric hydroxide to a dependence on hydrogen bond rearrangement. It should be noted that V_{max}/K_m includes the bimolecular encounter of substrate and enzyme, up to the first irreversible step (hydrogen atom abstraction), but V_{max} includes steps after enzyme substrate complex formation, and therefore, the SIE observed for V_{max} and V_{max}/K_m could be from the same step or from different steps.

Identical solvent dependence studies, with 5(S)-HpETE as a substrate, were also performed (Table 4). Interestingly, the V_{max} SIE for 5(S)-HpETE epoxidation (V_{max} SIE = 0.81 ± 0.1) was markedly different from that for AA (V_{max} SIE = 1.8 ± 0.2). This result clearly demonstrates an inverse SIE for 5(S)-HpETE epoxidation and indicates the participation of the Fe(III)−OH moiety in the hydrogen abstraction mechanism as a contributor to the rate-limiting step (*vide infra*). Adding ATP, with 5(S)-HpETE as the substrate, increased the epoxidation SIE to 2.6 ± 0.3. This increase in SIE is nearly identical to that with AA as a substrate, showing that both processes, AA hydroperoxidation and 5(S)-HpETE epoxidation, display an ATP-induced increase in SIE, suggesting a shift in their rate-limiting step to being more dependent on hydrogen bond rearrangement and less on the hydrogen atom abstraction by the Fe(III)−OH moiety.

For the V_{max}/K_m data, the 5(S)-HpETE epoxidation SIE is 0.49 ± 0.09. This value is similar to that seen previously for AA hydroperoxidation (SIE = 0.66 ± 0.3) and indicates that the rate-limiting step of V_{max}/K_m, for both AA hydroperoxidation and 5(S)-HpETE epoxidation, is dominated by the hydrogen atom abstraction of the Fe(III)−OH moiety. After addition of ATP, the 5(S)-HpETE epoxidation SIE increased to 1.2 ± 0.2, similar to the increase seen for the AA hydroperoxidation (SIE = 1.8 ± 0.6). This is consistent with a change in the rate-limiting step to being more dependent on hydrogen bond rearrangement and less on hydrogen atom abstraction. Considering that ATP activates both hydroperoxidation and epoxidation to a similar extent and in a similar manner, it is reasonable that for both processes, ATP increases the rate of hydrogen atom abstraction and hence lowers its contribution to the rate-limiting step.

In summary, the SIE results described above indicate that both hydrogen atom abstraction and hydrogen bond rearrangement are important rate-limiting steps for AA hydroperoxidation and 5(S)-HpETE epoxidation. However, the importance of hydrogen atom abstraction in the rate-limiting step increases for epoxidation and could explain the rate for epoxidation being slower than that for hydroperoxidation (*vide infra*). In addition, the ATP-induced allosteric effect changes the solvent dependency of the rate-limiting step for both hydroperoxidation and epoxidation, which cannot be explained by an ATP-induced stabilization of the 5-LOX protein structure.[31] Rather, the changes in SIE with the addition of ATP suggest a shift in the rate-limiting step toward hydrogen bond rearrangement relative to hydrogen atom abstraction for

both hydroperoxidation and epoxidation. Unfortunately, it could not determine if ATP affects hydrogen atom abstraction directly, because isotopically labeled AA is not readily available.

Viscosity Effects of the Hydroperoxidation and Epoxidation Kinetics. To further probe the nature of the rate-limiting step, viscosity experiments in dextrose ($\eta/\eta^{\circ} = 1$ and 3) were performed in the absence and presence of 200 μM ATP (Table 5). The $(V_{max}/K_m^{\circ})/(V_{max}/K_m)$ for AA substrate was calculated to be 1.5 ± 0.3 without ATP and 1.2 ± 0.2 with ATP, where V_{max}/K_m° has an η/η° of 1 and V_{max}/K_m has an η/η° of 3. These data indicate that the rate of substrate capture is not diffusion-controlled, with or without ATP. However, it is interesting to note that V_{max}°/V_{max} increased from 1.0 ± 0.1 to 1.6 ± 0.2 upon ATP activation. Because there is no viscosity effect seen for V_{max}/K_m, these data are best explained by decreased translational diffusion rates and/or conformational changes upon substrate binding,[62−64] the latter being consistent with the SIE results.

In contrast to the viscosity effect with AA as the substrate, an inverse viscosity effect can be seen on V_{max}/K_m with 5(S)-HpETE as the substrate $[(V_{max}/K_m^{\circ})/(V_{max}/K_m) = 0.65 \pm 0.1]$. Considering there is no viscosity effect observed under the same conditions for the faster reaction of 5-LOX and AA, the inverse viscosity effect on V_{max}/K_m with 5(S)-HpETE appears to arise through a different mechanism. A change in the dielectric environment[65] could result in an inverse effect, but the dielectric constant of water (~80) is reduced by only 10% with the addition of 30% by mass dextrose.[66] Moreover, the finding that this inverse viscosity effect is removed by the addition of ATP also suggests dielectric constants are not inducing the effect. Experiments with PEG-8000 were attempted to confirm that the viscosity effect is independent of a change in dielectric constants; however, PEG was observed to inactivate 5-LOX, and thus, no conclusion was possible (data not shown). The only other hypothesis for the inverse viscosity effect on $(V_{max}/K_m^{\circ})/(V_{max}/K_m)$ is due to a partially rate-determining conformational change during catalysis,[60] which is supported by the fact that the SIE results also indicate a conformational change. Upon addition of ATP, the $(V_{max}/K_m^{\circ})/(V_{max}/K_m)$ viscosity effect with 5(S)-HpETE as a substrate becomes 1.6 ± 0.4. Given the slow rate of 5(S)-HpETE epoxidation relative to AA hydroperoxidation, and the fact that no viscosity effect was seen for AA hydroperoxidation, the normal viscosity effect on 5(S)-HpETE V_{max}/K_m induced by ATP is most likely not due to a diffusion-controlled mechanism. Therefore, the small $(V_{max}/K_m^{\circ})/(V_{max}/K_m)$ viscosity effect with ATP may possibly be due to a conformational change during catalysis. The V_{max}°/V_{max} viscosity effect did not change upon addition of ATP (1.0 ± 0.2 to 1.3 ± 0.2), indicating diffusion is not rate-limiting, with or without ATP. It should be noted that only dextrose allowed for viscosity measurements. It is typical of LOX isozymes to be sensitive to high concentrations of viscogens;[47,60] however, the data would engender more confidence if another viscogen could manifest similar results. Future experiments are needed to probe the nature of the viscogen effect further.

■ CONCLUSION

It has been known in the literature for many years that 5-LOX has two catalytic functions, hydroperoxidation of AA (oxidation of PUFA) and epoxidation of 5(S)-HpETE (dehydration of hydroperoxide), but a detailed kinetic investigation comparing these two processes has never been undertaken. In the work presented here, we demonstrate that the V_{max} of 5(S)-HpETE epoxidation is 3-fold slower than the V_{max} of AA hydroperoxidation and that the corresponding V_{max}/K_m is 23-fold slower, indicating that both the rate of substrate capture and the rate of product release are less efficient for epoxidation than for hydroperoxidation. These rate differences could be due to the fact that the hydrogen atom is abstracted from C7 for hydroperoxidation of AA, as opposed to C10 for epoxidation of 5(S)-HpETE, as discussed in the introductory section (Figure 2). This hypothesis is supported by the SIE results, which indicate a stronger dependence on hydrogen atom abstraction for epoxidation than hydroperoxidation. In addition, if one measures the rate of epoxidation of endogenous and exogenous 5(S)-HpETE [i.e., 5(S)-HpETE generated *in situ* from AA and 5(S)-HpETE bound directly, respectively], one observes that their V_{max} values are the same. However, there is a 9-fold larger V_{max}/K_m for endogenous 5(S)-HpETE than for 5(S)-HpETE epoxidation. Considering that the V_{max} is the same for both processes, the rate difference appears to be due to a difference in a microscopic rate constant before hydrogen atom abstraction, possibly a structural rearrangement [k_3 for hydroperoxidation of AA and k_7 for epoxidation of 5(S)-HpETE]. In the recently determined crystal structure for human 5-LOX, a unique FY cork feature is observed that blocks one possible entrance to the active site.[32] We hypothesize that a difference in the rearrangement of the FY cork could be the source of the kinetic difference between AA and 5(S)-HpETE binding, highlighting future research directions for studying the epoxidation mechanism. Importantly, these results indicate that 5-LOX has overcome a significant catalytic barrier of epoxidation by retaining the 5(S)-HpETE in its active site for sequential epoxidation and not binding free 5(S)-HpETE directly.

Along this same line of investigation, it was determined that ATP activates the V_{max} of AA (4.9-fold) and the V_{max} of 5(S)-HpETE by a similar degree (4.8-fold). However, ATP activates the V_{max}/K_m to a lesser extent [1.7-fold for AA and 3.9-fold for 5(S)-HpETE], indicating ATP affects substrate capture and product release differently. Further titration of 5-LOX with ATP yielded hyperbolic kinetic parameters supporting the similarity between the activation of hydroperoxidation and epoxidation. Both processes displayed similar V-type activation, but the extent of K-type inhibition was greater with AA as the substrate, resulting in a greater activation for V_{max}/K_m for 5(S)-HpETE.

Inverse V_{max}/K_m SIE values observed for 5-LOX indicate the rate-limiting step for substrate capture is dominated by the hydrogen atom abstraction by the Fe(III)−OH moiety (k_5 for hydroperoxidation and k_{11} for epoxidation). However, ATP shifts the inverse V_{max}/K_m SIE for both AA and 5(S)-HpETE to normal SIE values, indicating an increased dependence of the rate-limiting step on solvent. Given the previous assignment of the SIE to hydrogen bond rearrangement for other LOX isozymes,[45−48,53] it appears that addition of ATP increases the dependence of the rate-limiting step on hydrogen bond rearrangement (k_3 and k_7) relative to hydrogen atom abstraction (k_5 and k_{11}). Considering that neither mechanism is limited by substrate diffusion but both substrate capture rates are limited by hydrogen atom abstraction (inverse SIE), it appears that the 23-fold faster rate for hydroperoxidation is due to an increased rate of hydrogen atom abstraction compared to the rate of epoxidation. In addition, it appears that ATP increases the rate of hydrogen atom abstraction, such that its contribution to the rate-limiting step is decreased. This hypothesis is remarkable because the position of the abstracted hydrogen atom for hydroperoxidation and epoxidation is distinct (C7 and C10, respectively), and the overall structure of the substrates is also distinct [AA vs 5(S)-HpETE]. However, subtle changes in the positioning of the abstracted hydrogen relative to the Fe(III)−OH moiety have an effect on LOX rates,[47,53] and therefore, substrate differences and/or addition of ATP would likely affect the rate of 5-LOX. We are currently investigating the molecular mechanism of ATP activation further to gain molecular insight into how the rate of hydrogen atom abstraction is increased.

With respect to the larger implications of these ATP results, 5-LOX has a unique role in the inflammatory response by catalyzing the formation of potent pro- and anti-inflammatory molecules, and as such, the cell has devised several strategies for regulating its control.[8,19,21,31,52,67] Along these lines, we note that ATP has a well-established role as an upregulated mediator in inflammation[68−70] and that extracellular ATP is measured at elevated levels for patients suffering from inflammatory diseases, such as chronic obstructive pulmonary disease (COPD) and emphysema, which are known to involve leukotrienes as causal factors in their pathology.[71−76] Lommatzsch et al. recently established that ATP concentrations in bronchoalveolar lavage fluid increased from <10 μM in a control group of patients to >300 μM in patients with increasing stages of COPD. They also presented *in vitro* results suggesting that increasing concentrations of extracellular ATP, from 1 to 100 μM, increased the chemotactic index of human neutrophils, an effect that saturated and resisted any further changes even when probed with 1000 μM extracellular ATP.[72] While a direct link to 5-LOX activity was not tested, we note that these results correlate with our measured K_i of ATP-induced activation for 5-LOX (∼10 μM), suggesting a possible connection between the increasing chemotactic index and ATP-induced activation of 5-LOX in disease. There is also evidence of intracellular compartmentalization of ATP itself up to low millimolar concentrations[77] and for high micromolar amounts of ATP being released extracellularly from HEK293 and ACN neuroblastoma cells through nonlytic ATP release,[78] further demonstrating that the concentration of ATP necessary for ATP-induced activation is biologically relevant. We reason that these divergent lines of evidence could suggest that the ATP-induced allosteric effect of 5-LOX we have characterized herein may be another biologically relevant form of 5-LOX regulation through which inflammation control can be modulated. The distinction between extracellular and intracellular ATP is an important one, and while ATP is thought to be released from neutrophils,[74] 5-LOX activation would still require an elevated intracellular ATP concentration prior to release. The critical question is whether the ATP concentration in the 5-LOX-localized cellular compartment is changing as the experiments described above predict, suggesting future directions for *in vivo* research.

AUTHOR INFORMATION

Corresponding Author

*E-mail: tholman@chemistry.ucsc.edu. Phone: (831) 459-5884. Fax: (831) 459-2935.

Notes

The authors declare no competing financial interest.

ACKNOWLEDGMENTS

ABBREVIATIONS

AA, arachidonic acid; CLP, coactosin-like protein; CMC, critical micelle concentration; 5,12-DiHETE, 5,12-dihydroxy-6(E),8(E),10(E),14(Z)-eicosatetraenoic acid; FLAP, 5-LOX-activating protein; 5(S)-HETE, 5(S)-hydroxy-6(E),8(Z),11-(Z),14(Z)-eicosatetraenoic acid; 5(S)-HpETE, 5(S)-hydroperoxy-6(E),8(Z),11(Z),14(Z)-eicosatetraenoic acid; 13(S)-HpODE, 13(S)-hydroperoxy-9(Z),11(E)-octadecadienoic acid; k_{cat}, rate constant for product release; k_{cat}/K_m, rate constant for substrate capture; LOX, lipoxygenase; 5-LOX, human 5-lipoxygenase; 12-LOX, human platelet 12-lipoxygenase; 15-LOX-1, human reticulocyte 15-lipoxygenase-1; 15-LOX-2, human epithelial 15-lipoxygenase-2; soybean LOX-1, soybean lipoxygenase-1; LTA$_4$, leukotriene A$_4$; LTB$_4$, leukotriene B$_4$; LXA$_4$, lipoxin A$_4$; LXB$_4$, lipoxin B$_4$; PLAT, polycystin-1/lipoxygenase/α-toxin; PMNL, polymorphonuclear leukocyte; PUFA, polyunsaturated fatty acid; RvD1, resolvin D1; RvE1, resolvin E1; SIE, solvent isotope effect; hydroperoxidation, oxidation of AA; epoxidation, dehydration of a hydroperoxide to form an epoxide; endogenous 5(S)-HpETE, 5(S)-HpETE generated *in situ* from AA; exogenous 5(S)-HpETE, free 5(S)-HpETE in solution.

REFERENCES

(1) Jakschik, B. A., and Lee, L. H. (1980) Enzymatic assembly of slow reacting substance. *Nature 287*, 51−52.

(2) Rådmark, O. (2002) Arachidonate 5-lipoxygenase. *Prostaglandins Other Lipid Mediators 68−69*, 211−234.

(3) Samuelsson, B. (1983) Leukotrienes: Mediators of immediate hypersensitivity reactions and inflammation. *Science 220*, 568−575.

(4) Shimizu, T., Radmark, O., and Samuelsson, B. (1984) Enzyme with dual lipoxygenase activities catalyzes leukotriene A4 synthesis from arachidonic acid. *Proc. Natl. Acad. Sci. U.S.A. 81*, 689−693.

(5) Borgeat, P., and Samuelsson, B. (1979) Metabolism of arachidonic acid in polymorphonuclear leukocytes. Structural analysis of novel hydroxylated compounds. *J. Biol. Chem. 254*, 7865−7869.

(6) Ueda, N., Yamamoto, S., Oates, J. A., and Brash, A. R. (1986) Stereoselective hydrogen abstraction in leukotriene A4 synthesis by purified 5-lipoxygenase of porcine leukocytes. *Prostaglandins 32*, 43−48.

(7) Fitzpatrick, F., Liggett, W., McGee, J., Bunting, S., Morton, D., and Samuelsson, B. (1984) Metabolism of leukotriene A4 by human erythrocytes. A novel cellular source of leukotriene B4. *J. Biol. Chem. 259*, 11403−11407.

(8) Sala, A., Folco, G., and Murphy, R. C. (2010) Transcellular biosynthesis of eicosanoids. *Pharmacol. Rep. 62*, 503−510.

(9) Serhan, C. N. (2002) Lipoxins and aspirin-triggered 15-epi-lipoxin biosynthesis: An update and role in anti-inflammation and pro-resolution. *Prostaglandins Other Lipid Mediators 68−69*, 433−455.

(10) Serhan, C. N., and Savill, J. (2005) Resolution of inflammation: The beginning programs the end. *Nat. Immunol. 6*, 1191−1197.

(11) Rouzer, C. A., and Samuelsson, B. (1987) Reversible, calcium-dependent membrane association of human leukocyte 5-lipoxygenase. *Proc. Natl. Acad. Sci. U.S.A. 84*, 7393−7397.

(12) Hammarberg, T., and Radmark, O. (1999) 5-Lipoxygenase binds calcium. *Biochemistry 38*, 4441−4447.

(13) Allard, J. B., and Brock, T. G. (2005) Structural organization of the regulatory domain of human 5-lipoxygenase. *Curr. Protein Pept. Sci. 6*, 125−131.

(14) Reddy, K. V., Hammarberg, T., and Radmark, O. (2000) Mg²⁺ activates 5-lipoxygenase in vitro: Dependency on concentrations of phosphatidylcholine and arachidonic acid. *Biochemistry 39*, 1840−1848.

(15) Noguchi, M., Miyano, M., Matsumoto, T., and Noma, M. (1994) Human 5-lipoxygenase associates with phosphatidylcholine liposomes and modulates LTA4 synthetase activity. *Biochim. Biophys. Acta 1215*, 300−306.

(16) Hill, E., Maclouf, J., Murphy, R. C., and Henson, P. M. (1992) Reversible membrane association of neutrophil 5-lipoxygenase is accompanied by retention of activity and a change in substrate specificity. *J. Biol. Chem. 267*, 22048−22053.

(17) Evans, J. F., Ferguson, A. D., Mosley, R. T., and Hutchinson, J. H. (2008) What's all the FLAP about?: 5-Lipoxygenase-activating protein inhibitors for inflammatory diseases. *Trends Pharmacol. Sci. 29*, 72−78.

(18) Dixon, R. A., Diehl, R. E., Opas, E., Rands, E., Vickers, P. J., Evans, J. F., Gillard, J. W., and Miller, D. K. (1990) Requirement of a 5-lipoxygenase-activating protein for leukotriene synthesis. *Nature 343*, 282−284.

(19) Rakonjac, M., Fischer, L., Provost, P., Werz, O., Steinhilber, D., Samuelsson, B., and Rådmark, O. (2006) Coactosin-like protein supports 5-lipoxygenase enzyme activity and up-regulates leukotriene A4 production. *Proc. Natl. Acad. Sci. U.S.A. 103*, 13150−13155.

(20) Esser, J., Rakonjac, M., Hofmann, B., Fischer, L., Provost, P., Schneider, G., Steinhilber, D., Samuelsson, B., and Rådmark, O. (2009) Coactosin-like protein functions as a stabilizing chaperone for 5-lipoxygenase: Role of tryptophan 102. *Biochem. J. 425*, 265−274.

(21) Newcomer, M. E., and Gilbert, N. C. (2010) Location, location, location: Compartmentalization of early events in leukotriene biosynthesis. *J. Biol. Chem. 285*, 25109−25114.

(22) Peters-Golden, M., and Brock, T. G. (2001) Intracellular compartmentalization of leukotriene synthesis: Unexpected nuclear secrets. *FEBS Lett. 487*, 323−326.

(23) Brock, T. G. (2005) Regulating leukotriene synthesis: The role of nuclear 5-lipoxygenase. *J. Cell. Biochem. 96*, 1203−1211.

(24) Luo, M., Flamand, N., and Brock, T. G. (2006) Metabolism of arachidonic acid to eicosanoids within the nucleus. *Biochim. Biophys. Acta 1761*, 618−625.

(25) Lepley, R. A., Muskardin, D. T., and Fitzpatrick, F. A. (1996) Tyrosine kinase activity modulates catalysis and translocation of cellular 5-lipoxygenase. *J. Biol. Chem. 271*, 6179−6184.

(26) Häfner, A.-K., Cernescu, M., Hofmann, B., Ermisch, M., Hörnig, M., Metzner, J., Schneider, G., Brutschy, B., and Steinhilber, D. (2011) Dimerization of human 5-lipoxygenase. *Biol. Chem. 392*, 1097−1111.

(27) Ochi, K., Yoshimoto, T., Yamamoto, S., Taniguchi, K., and Miyamoto, T. (1983) Arachidonate 5-lipoxygenase of guinea pig peritoneal polymorphonuclear leukocytes. Activation by adenosine 5′-triphosphate. *J. Biol. Chem. 258*, 5754−5758.

(28) Rouzer, C. A., Thornberry, N. A., and Bull, H. G. (1988) Kinetic effects of ATP and two cellular stimulatory components on human leukocyte 5-lipoxygenase. *Ann. N.Y. Acad. Sci. 524*, 1−11.

(29) Noguchi, M., Miyano, M., and Matsumoto, T. (1996) Physiochemical characterization of ATP binding to human 5-lipoxygenase. *Lipids 31*, 367−371.

(30) Aharony, D., and Stein, R. L. (1986) Kinetic mechanism of guinea pig neutrophil 5-lipoxygenase. *J. Biol. Chem. 261*, 11512–11519.

(31) Rådmark, O., and Samuelsson, B. (2005) Regulation of 5-lipoxygenase enzyme activity. *Biochem. Biophys. Res. Commun. 338*, 102–110.

(32) Gilbert, N. C., Bartlett, S. G., Waight, M. T., Neau, D. B., Boeglin, W. E., Brash, A. R., and Newcomer, M. E. (2011) The structure of human 5-lipoxygenase. *Science 331*, 217–219.

(33) Knapp, M. J., and Klinman, J. P. (2003) Kinetic studies of oxygen reactivity in soybean lipoxygenase-1. *Biochemistry 42*, 11466–11475.

(34) Jin, J., Zheng, Y., Boeglin, W. E., and Brash, A. R. (2012) Biosynthesis, isolation, and NMR analysis of leukotriene A epoxides: Substrate chirality as a determinant of the cis or trans epoxide configuration. *J. Lipid Res. 54*, 754–761.

(35) Robinson, S. J., Hoobler, E. K., Riener, M., Loveridge, S. T., Tenney, K., Valeriote, F. A., Holman, T. R., and Crews, P. (2009) Using enzyme assays to evaluate the structure and bioactivity of sponge-derived meroterpenes. *J. Nat. Prod. 72*, 1857–1863.

(36) Mogul, R., and Holman, T. R. (2001) Inhibition studies of soybean and human 15-lipoxygenases with long-chain alkenyl sulfate substrates. *Biochemistry 40*, 4391–4397.

(37) Mogul, R., Johansen, E., and Holman, T. R. (2000) Oleyl sulfate reveals allosteric inhibition of soybean lipoxygenase-1 and human 15-lipoxygenase. *Biochemistry 39*, 4801–4807.

(38) Joshi, N., Hoobler, E. K., Perry, S., Diaz, G., Fox, B. G., and Holman, T. R. (2013) Kinetic and structural investigations into the allosteric and pH effect on substrate specificity of human epithelial 15-lipoxygenase-2. *Biochemistry 52*, 8026–8035.

(39) McAuley, W. J., Jones, D. S., and Kett, V. L. (2009) Characterisation of the interaction of lactate dehydrogenase with Tween-20 using isothermal titration calorimetry, interfacial rheometry and surface tension measurements. *J. Pharm. Sci. 98*, 2659–2669.

(40) Wiseman, J. S., Skoog, M. T., Nichols, J. S., and Harrison, B. L. (1987) Kinetics of leukotriene A4 synthesis by 5-lipoxygenase from rat polymorphonuclear leukocytes. *Biochemistry 26*, 5684–5689.

(41) Petrich, K., Ludwig, P., Kuhn, H., and Schewe, T. (1996) The suppression of 5-lipoxygenation of arachidonic acid in human polymorphonuclear leucocytes by the 15-lipoxygenase product (15S)-hydroxy-(5Z,8Z,11Z,13E)-eicosatetraenoic acid: Structure-activity relationship and mechanism of action. *Biochem. J. 314*, 911–916.

(42) Deems, R., Buczynski, M. W., Bowers-Gentry, R., Harkewicz, R., and Dennis, E. A. (2007) Detection and quantitation of eicosanoids via high performance liquid chromatography-electrospray ionization-mass spectrometry. *Methods Enzymol. 432*, 59–82.

(43) Derogis, P. B. M. C., Freitas, F. P., Marques, A. S. F., Cunha, D., Appolinário, P. P., de Paula, F., Lourenço, T. C., Murgu, M., Di Mascio, P., Medeiros, M. H. G., and Miyamoto, S. (2013) The development of a specific and sensitive LC-MS-based method for the detection and quantification of hydroperoxy- and hydroxydocosahexaenoic acids as a tool for lipidomic analysis. *PLoS One 8*, e77561.

(44) Lewis, E. R., Johansen, E., and Holman, T. R. (1999) Large competitive kinetic isotope effects in human 15-lipoxygenase catalysis measured by a novel HPLC method. *J. Am. Chem. Soc. 121*, 1395–1396.

(45) Wecksler, A. T., Jacquot, C., van der Donk, W. A., and Holman, T. R. (2009) Mechanistic investigations of human reticulocyte 15- and platelet 12-lipoxygenases with arachidonic acid. *Biochemistry 48*, 6259–6267.

(46) Segraves, E. N., and Holman, T. R. (2003) Kinetic investigations of the rate-limiting step in human 12- and 15-lipoxygenase. *Biochemistry 42*, 5236–5243.

(47) Glickman, M. H., and Klinman, J. P. (1995) Nature of rate-limiting steps in the soybean lipoxygenase-1 reaction. *Biochemistry 34*, 14077–14092.

(48) Wecksler, A. T., Kenyon, V., Garcia, N. K., Deschamps, J. D., van der Donk, W. A., and Holman, T. R. (2009) Kinetic and structural investigations of the allosteric site in human epithelial 15-lipoxygenase-2. *Biochemistry 48*, 8721–8730.

(49) Skorey, K. I., and Gresser, M. J. (1998) Calcium is not required for 5-lipoxygenase activity at high phosphatidyl choline vesicle concentrations. *Biochemistry 37*, 8027–8034.

(50) Puustinen, T., Scheffer, M. M., and Samuelsson, B. (1987) Endogenously generated 5-hydroperoxyeicosatetraenoic acid is the preferred substrate for human leukocyte leukotriene A4 synthase activity. *FEBS Lett. 217*, 265–268.

(51) Reinhart, G. D. (2004) Quantitative analysis and interpretation of allosteric behavior. *Methods Enzymol. 380*, 187–203.

(52) Rådmark, O., Werz, O., Steinhilber, D., and Samuelsson, B. (2007) 5-Lipoxygenase: Regulation of expression and enzyme activity. *Trends Biochem. Sci. 32*, 332–341.

(53) Glickman, M. H., Wiseman, J. S., and Klinman, J. P. (1994) Extremely large isotope effects in the soybean lipoxygenase-linoleic acid reaction. *J. Am. Chem. Soc. 116*, 793–794.

(54) Borgeat, P., Hamberg, M., and Samuelsson, B. (1976) Transformation of arachidonic acid and homo-γ-linolenic acid by rabbit polymorphonuclear leukocytes. Monohydroxy acids from novel lipoxygenases. *J. Biol. Chem. 251*, 7816–7820.

(55) Maas, R. L., Ingram, C. D., Taber, D. F., Oates, J. A., and Brash, A. R. (1982) Stereospecific removal of the DR hydrogen atom at the 10-carbon of arachidonic acid in the biosynthesis of leukotriene A4 by human leukocytes. *J. Biol. Chem. 257*, 13515–13519.

(56) Panossian, A., Hamberg, M., and Samuelsson, B. (1982) On the mechanism of biosynthesis of leukotrienes and related compounds. *FEBS Lett. 150*, 511–513.

(57) Schowen, K. B., and Schowen, R. L. (1982) Solvent isotope effects of enzyme systems. *Methods Enzymol. 87*, 551–606.

(58) Quinn, D. M., and Sutton, L. D. (1991) Theoretical basis and mechanistic utility of solvent isotope effects. *Enzyme mechanism from isotope effects* (Cook, P. F., Ed.) pp 73–126, CRC Press, Boca Raton, FL.

(59) Bott, R. R., Chan, G., Domingo, B., Ganshaw, G., Hsia, C. Y., Knapp, M., and Murray, C. J. (2003) Do enzymes change the nature of transition states? Mapping the transition state for general acid-base catalysis of a serine protease. *Biochemistry 42*, 10545–10553.

(60) Raber, M. L., Freeman, M. F., and Townsend, C. A. (2009) Dissection of the stepwise mechanism to β-lactam formation and elucidation of a rate-determining conformational change in β-lactam synthetase. *J. Biol. Chem. 284*, 207–217.

(61) Tomchick, D. R., Phan, P., Cymborowski, M., Minor, W., and Holman, T. R. (2001) Structural and functional characterization of second-coordination sphere mutants of soybean lipoxygenase-1. *Biochemistry 40*, 7509–7517.

(62) Pocker, Y., and Janjić, N. (1987) Enzyme kinetics in solvents of increased viscosity. Dynamic aspects of carbonic anhydrase catalysis. *Biochemistry 26*, 2597–2606.

(63) Pocker, Y., and Janjić, N. (1988) Origin of viscosity effects in carbonic anhydrase catalysis. Kinetic studies with bulky buffers at limiting concentrations. *Biochemistry 27*, 4114–4120.

(64) Kanosue, Y., Kojima, S., and Ohkata, K. (2004) Influence of solvent viscosity on the rate of hydrolysis of dipeptides by carboxypeptidase Y. *J. Phys. Org. Chem. 17*, 448–457.

(65) Almagor, A., Yedgar, S., and Gavish, B. (1992) Viscous cosolvent effect on the ultrasonic absorption of bovine serum albumin. *Biophys. J. 61*, 480–486.

(66) Malmberg, C. G., and Maryott, A. A. (1950) Dielectric constants of aqueous solutions of dextrose and sucrose. *J. Res. Natl. Bur. Stand. (U.S.) 45*, 299–303.

(67) Mandal, A. K., Jones, P. B., Bair, A. M., Christmas, P., Miller, D., Yamin, T.-T. D., Wisniewski, D., Menke, J., Evans, J. F., Hyman, B. T., Bacskai, B., Chen, M., Lee, D. M., Nikolic, B., and Soberman, R. J. (2008) The nuclear membrane organization of leukotriene synthesis. *Proc. Natl. Acad. Sci. U.S.A. 105*, 20434–20439.

(68) Bodin, P., and Burnstock, G. (1998) Increased release of ATP from endothelial cells during acute inflammation. *Inflammation Res. 47*, 351–354.

(69) Burnstock, G., Brouns, I., Adriaensen, D., and Timmermans, J. P. (2012) Purinergic signaling in the airways. *Pharmacol. Rev. 64*, 834–868.

(70) Gourine, A. V., Dale, N., Llaudet, E., Poputnikov, D. M., Spyer, K. M., and Gourine, V. N. (2007) Release of ATP in the central nervous system during systemic inflammation: Real-time measurement in the hypothalamus of conscious rabbits. *J. Physiol. 585*, 305–316.

(71) Esther, C. R., Alexis, N. E., and Picher, M. (2011) Regulation of airway nucleotides in chronic lung diseases. *Subcell. Biochem. 55*, 75–93.

(72) Lommatzsch, M., Cicko, S., Müller, T., Lucattelli, M., Bratke, K., Stoll, P., Grimm, M., Dürk, T., Zissel, G., Ferrari, D., Di Virgilio, F., Sorichter, S., Lungarella, G., Virchow, J. C., and Idzko, M. (2010) Extracellular adenosine triphosphate and chronic obstructive pulmonary disease. *Am. J. Respir. Crit. Care Med. 181*, 928–934.

(73) Mortaz, E., Folkerts, G., Nijkamp, F. P., and Henricks, P. A. J. (2010) ATP and the pathogenesis of COPD. *Eur. J. Pharmacol. 638*, 1–4.

(74) Mortaz, E., Braber, S., Nazary, M., Givi, M. E., Nijkamp, F. P., and Folkerts, G. (2009) ATP in the pathogenesis of lung emphysema. *Eur. J. Pharmacol. 619*, 92–96.

(75) Rorke, S. (2002) Role of cysteinyl leukotrienes in adenosine 5′-monophosphate induced bronchoconstriction in asthma. *Thorax 57*, 323–327.

(76) Idzko, M., Hammad, H., van Nimwegen, M., Kool, M., Willart, M. A. M., Muskens, F., Hoogsteden, H. C., Luttmann, W., Ferrari, D., Di Virgilio, F., Virchow, J. C., and Lambrecht, B. N. (2007) Extracellular ATP triggers and maintains asthmatic airway inflammation by activating dendritic cells. *Nat. Med. 13*, 913–919.

(77) Miller, D. S., and Horowitz, S. B. (1986) Intracellular compartmentalization of adenosine triphosphate. *J. Biol. Chem. 261*, 13911–13915.

(78) Pellegatti, P., Falzoni, S., Pinton, P., Rizzuto, R., and Di Virgilio, F. (2005) A novel recombinant plasma membrane-targeted luciferase reveals a new pathway for ATP secretion. *Mol. Biol. Cell 16*, 3659–3665.

(79) Hamberg, M., and Hamberg, G. (1980) On the mechanism of the oxygenation of arachidonic acid by human platelet lipoxygenase. *Biochem. Biophys. Res. Commun. 95*, 1090–1097.